

Mechanism of Hydrogen Sorption in Single-Walled Carbon Nanotubes

Hansong Cheng,* Guido P. Pez, and Alan C. Cooper

Computational Modeling Center and Corporate Science and Technology Center, Air Products and Chemicals, Inc.
7201 Hamilton Boulevard,
Allentown, Pennsylvania 18195-1501

Received January 9, 2001

Revised Manuscript Received April 24, 2001

The development of novel materials that are capable of effectively storing molecular hydrogen is of great current interest, stimulated by advances in proton exchange membrane (PEM) fuel cell technology. Recently, Dillon, Heben, et al. reported that single-walled carbon nanotubes (SWNT's) could reversibly adsorb 5–10 wt % H₂ at near-ambient conditions.¹ The reported heat (enthalpy) of adsorption was -4.7 kcal mol⁻¹—much greater than the ca. -1 kcal mol⁻¹ of conventional high-surface-area activated carbons or graphite.² Subsequently, several computational studies, based upon classical simulations, suggested that while weak interactions between H₂ and SWNT's do exist, the H₂ adsorption energy, and hence the near-ambient-temperature storage capacity of carbon nanotubes, falls far short from the reported experimental enthalpy.³ Indeed, whether SWNT's are capable of adsorbing and storing enough H₂ for practical applications remains a subject of considerable controversy.⁴

Here, by analysis of quantum-mechanical molecular dynamics (MD) simulations,⁵ we describe a mechanism that yields calculated energies of adsorption which are comparable to, and can surpass, the reported¹ experimental heat of adsorption for H₂ on SWNT's. Partial electron-transfer interaction between instantaneously distorted carbon atoms in the SWNT wall and H₂ is proposed to be the primary phenomenon responsible for the unique strength of the hydrogen-SWNT adsorption energy.

SWNT's prepared by the carbon-arc⁶ and laser-ablation⁷ methods typically exist in a trigonal two-dimensional lattice (i.e. “ropes” or “bundles”) of nanotubes which predominantly have an “armchair” architecture and a narrow diameter range (ca. 12–14 Å, corresponding to 9,9 and 10,10 nanotubes⁸). Therefore, for our MD simulations, we have selected a unit cell within a trigonal SWNT lattice comprised of 9,9 nanotubes (diameter 11.89 Å).⁹ Upon energy minimization of the SWNT lattice, the potential energy surface near the equilibrium point was found to be

(1) Dillon, A. C.; Jones, K. M.; Bekkedahl, T. A.; Kiang, C. H.; Bethune, D. S.; Heben, M. J. *Nature* **1997**, *386*, 377.

(2) Pace, E. L.; Siebert, A. R. *J. Phys. Chem.* **1959**, *63*, 1398.

(3) (a) Wang, Q.; Johnson, J. K. *J. Chem. Phys.* **1999**, *110*, 557. (b) Stan, G.; Cole, M. W. *J. Low Temp. Phys.* **1998**, *110*, 539. (c) Williams, K. A.; Eklund, P. C. *Chem. Phys. Lett.* **2000**, *320*, 352.

(4) (a) Dresselhaus, M. S.; Williams, K. A.; Eklund, P. C. *Mater. Res., Bull.* **1999**, *24*, 45. (b) Ye, Y.; Ahn, C. C.; Witham, C.; Fultz, B.; Liu, J.; Rinzler, A. G.; Colbert, D.; Smith, K. A.; Smalley, R. E. *Appl. Phys. Lett.* **1999**, *74*, 2307.

(5) MD simulations were performed using the Vienna Ab initio Simulation Package^{5b} (VASP), which has been used successfully to model experimentally observed H₂ adsorption in KC₂₄ graphite at cryogenic temperatures.^{5c} (b) Kresse, G.; Hafner, J. *Phys. Rev. B* **1993**, *47*, 558. (c) Cheng, H.; Pez, G. P.; Kern, G.; Kresse, G.; Hafner, J. *J. Phys. Chem. B* **2001**, *105*, 736.

(6) Journet, C.; Maser, W. K.; Bernier, P.; Loiseau, A.; Lamy de la Chapelle, M.; Lefrant, S.; Deniard, P.; Lee, R.; Fischer, J. E. *Nature* **1997**, *388*, 756.

(7) Thess, A.; Lee, R.; Nikolaev, P.; Dai, H.; Petit, P.; Robert, J.; Xu, C.; Lee, Y. H.; Kim, S. G.; Rinzler, A. G.; Colbert, D. T.; Scuseria, G. E.; Tomanek, D.; Fischer, J. E.; Smalley, R. E. *Science* **1996**, *273*, 483.

(8) Dresselhaus, M. S.; Dresselhaus, G.; Eklund, P. C. *Science of Fullerenes and Carbon Nanotubes*; Academic Press: New York, 1996.

(9) Classical Monte Carlo simulations with rigid tubes have suggested that lattice structure may influence the magnitude of H₂ adsorption in SWNT's: Darkrim, F.; Levesque, D. *J. Phys. Chem. B* **2000**, *104*, 6773.

Table 1. The Energies (kcal mol⁻¹) of Adsorption of H₂ in SWNT's

temp, K	endohedral	exohedral
77	-3.94	-4.79
300	-7.51	-6.75
600	-3.86	-10.91

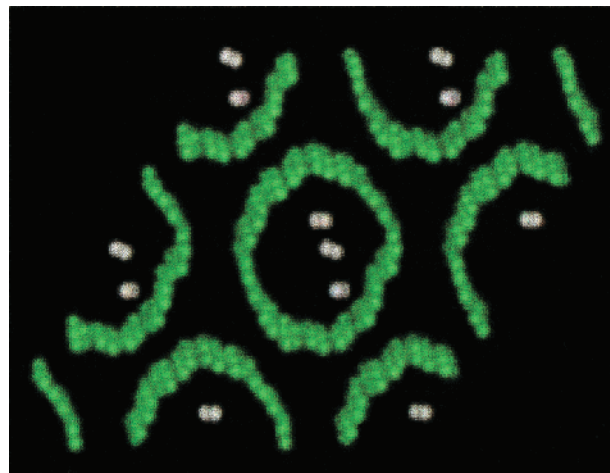


Figure 1. A representative time step during the MD simulation of endohedral H₂ adsorption at 300 K. The radial deformation of the SWNT wall and orientation of the H₂ molecules are illustrative of the dynamics observed throughout the simulation.

relatively flat. Significant changes of the lattice constants, >0.5 Å, resulted in only marginal changes in the lattice energy (<1 kcal mol⁻¹).

A fundamental issue concerning hydrogen adsorption in SWNT's is site selectivity; arrays of SWNT's with open ends may accommodate hydrogen in at least two sites: inside the nanotubes (endohedral adsorption) or in the interstitial pores formed between nanotubes (exohedral adsorption).

Time-averaged adsorption energies, over 5.0 ps, for endohedral and exohedral adsorption were calculated at 77, 300, and 600 K (Table 1). At 77 K, the calculations show a thermodynamic preference for adsorption in the smaller (ca. 4 Å) interstitial pores vs the endohedral pores.

The 600 K calculations suggest that exohedral adsorption is significantly more thermodynamically favorable and, remarkably, show the highest adsorption energy of any temperature.¹⁰ Our analysis reveals that the hydrogen molecules migrate within both of the endohedral/exohedral pores and, when proximal to the wall of the nanotube, are most often oriented toward the sites of greatest distortion (Figure 1).

The dynamic fluctuations induce localized, transient changes in the shape of the nanotube, creating regions of near planarity in the otherwise curved SWNT wall, and concomitant regions which contain very acute C–C–C bond angles. The global structural effect on the nanotubes is visualized as a dynamic bending and flexing of the overall nanotube, made possible within the SWNT lattice by the shallow potential energy surface near the equilibrium lattice structure. The flexibility of individual SWNT's, and ropes of SWNT's, which must occur by the

(10) Three H₂ molecules/108 carbon atoms were used in the unit cell for either exohedral or endohedral simulations (0.47 wt % hydrogen). The averaged adsorption energies described here approximate an upper limit for the strength of the H₂–SWNT interaction because the H₂ density is low compared to reported¹ experimental conditions. MD simulations with higher wt % densities of hydrogen in the unit cell have demonstrated a gradual decrease in average H₂ adsorption energies.^{10b} (b) Cheng, H.; Pez, G. P.; Cooper, A. C. Unpublished results.

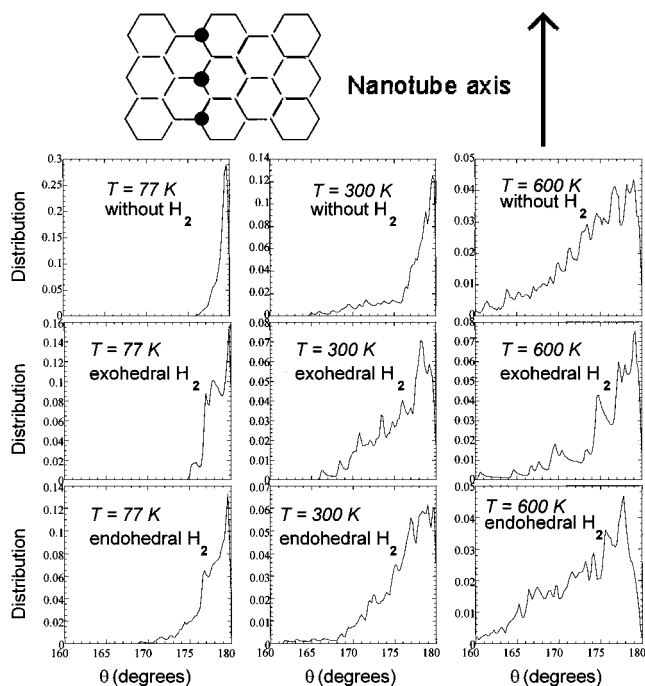


Figure 2. Longitudinal SWNT deformations at 77, 300, and 600 K as indicated by the distribution of C–C–C angles (θ) for the highlighted carbon atoms illustrated on a section of the SWNT wall. Each graph represents a distribution of C–C–C angle populations over 5000 steps of the 5.0 ps MD simulation. The longitudinal C–C–C angle of a perfectly circular and straight “armchair” SWNT is 180°.

compression of certain longitudinal C–C–C angles, has been verified experimentally by transmission electron microscopy of SWNT tori.¹¹ Bending and folding of SWNT's, resulting in distortion of radial C–C–C angles, has also been observed experimentally¹² and investigated using computational methods.¹³ The magnitude and range of nanotube distortions during our MD simulation are represented quantitatively using analysis of the angle between three selected, longitudinally oriented carbon atoms of the SWNT's (Figure 2). The population and range of distorted longitudinal angles ($<180^\circ$) are maximal in the presence of adsorbed hydrogen and at 600 K, leading to the observation of angles below 160°. The effect of temperature on SWNT deformations is clearly observed in the analysis of selected radial C–C–C angles (see Supporting Information), where the largest fluctuations are observed with, and without, adsorbed H₂ at 600 K.

(11) (a) Liu, J.; Dai, H.; Hafner, J. H.; Colbert, D. T.; Smalley, R. E. *Nature* **1997**, *385*, 780. (b) Martel, R.; Shea, H. R.; Avouris, P. *Nature* **1999**, *398*, 299.

(12) Kiang, C.-H.; Goddard, W. A., III; Beyers, R.; Bethune, D. S. *J. Phys. Chem.* **1996**, *100*, 3749.

(13) Gao, G.; Cagin, T.; Goddard, W. A., III *Nanotechnology* **1998**, *9*, 184.

The MD trajectory (Supporting Information) reveals that hydrogen-induced deformations of nanotubes facilitate the migration of hydrogen within the SWNT lattice. The potential energy barrier along the dynamic pathway between two interstitial pores increases as the molecules transit the narrow channel formed by neighboring nanotubes. Thus, migration from one interstitial pore to another is not indicated at 77 K, but is observed at 300 K and is facile at 600 K, due to a flattening of the nanotube walls when the transit of a hydrogen molecule occurs.

The atomistic quantum mechanical description of SWNT's used in our ab initio MD simulation reveals partial electron-transfer interactions of hydrogen with specific, highly distorted carbon atoms (very acute C–C–C bond angles) in the nanotube walls. The deviation from planarity, inherent in the curvature of a graphene sheet to form a SWNT and coupled with further distortion due to collisions with H₂ molecules, necessarily changes the hybridization of carbon from purely sp² (as in graphite) toward sp³, with a corresponding increased localization of electron density on the affected carbon atoms. Nanotube deformation has been shown to alter the electronic properties of SWNT's, which has been attributed to the change of the bonding configuration of mechanically distorted C atoms to sp³.¹⁴ During the observed interactions, the H₂ molecules are lengthened from the calculated gas-phase H–H bond distance of 0.75 Å and oriented “end-on” to the distorted carbon atom, characteristic of H₂ acting as an acceptor of electron density.¹⁵ Consistent with electron donation into the σ^* (antibonding) orbital of H₂, the distribution of $r_{\text{H-H}}$ is shifted toward longer H–H bond distances at the higher simulation temperatures, where the calculated adsorption energies are greatest. These enhanced electron-transfer interactions likely contribute to the higher energies of adsorption.

Finally, it is interesting to note that SWNT-gas contact, with a number of gases, has been found to alter electronic properties of SWNT.¹⁶ It is probable that perturbation of the nanotube structure and electron-transfer between distorted carbon atoms and certain gases play a role in these recent observations.

Acknowledgment. We thank J. Hafner, G. Kresse, and B. Peterson for helpful discussions and acknowledge Air Products and Chemicals, Inc. for encouraging this work and the publication of these results.

Supporting Information Available: Computational details, unit cell parameters, graphical representation of radial SWNT deformations at 77, 300, and 600 K, trajectory analysis of molecular dynamics simulation of endohedral and exohedral H₂ at 77, 300, and 600 K, and distribution of $r_{\text{H-H}}$ for endohedral and exohedral H₂ at 77, 300, and 600 K (PDF). This material is available free of charge via the Internet at <http://pubs.acs.org>.

JA0155231

(14) (a) Tomblor, T. W.; Zhou, C.; Alexseyev, L.; Kong, J.; Dai, H.; Liu, L.; Jayanthi, C. S.; Tang, M.; Wu, S.-Y. *Nature* **2000**, *405*, 769. (b) Liu, L.; Jayanthi, C. S.; Tang, M.; Wu, S.-Y.; Tomblor, T. W.; Zhou, C.; Alexseyev, L.; Kong, J.; Dai, H. *Phys. Rev. Lett.* **2000**, *84*, 4950.

(15) Sweany, R. L.; Ogden, J. S. *Inorg. Chem.* **1997**, *36*, 2523.

(16) (a) Collins, P. G.; Bradley, K.; Ishigami, M.; Zettl, A. *Science* **2000**, *287*, 1801. (b) Sumanasekera, G. U.; Adu, C. K. W.; Fang, S.; Eklund, P. C. *Phys. Rev. Lett.* **2000**, *85*, 1096.